Journal of the European Ceramic Society **10** (1992) 213–220

The Promise of EXAFS/EXELFS Spectroscopy for Structure Analysis in Ceramic Composites

E. Zschech, G. Binde & V. Klemm

Bergakademie Freiberg, Fachbereich Werkstoffwissenschaft, Gustav-Zeuner-Str. 3, 0-9200 Freiberg, Germany

(Received 13 February 1992; revised version received 10 April 1992; accepted 6 May 1992)

Abstract

Spectroscopic methods that are based on the elastic scattering of photoelectrons generated within the solid by an excitation process allow an element-specific analysis of materials. Information about the short-range order of ill-ordered regions in ceramic composites can be gained from a numerical analysis of EXAFS and EXELFS data. In particular, possibilities and problems to be expected for structure analysis of silicon oxycarbide matrices in composites fabricated by Active Filler Controlled Pyrolysis (AFCOP) are discussed. EXAFS spectroscopy gives an integral signal of the glass sample whereby the information depth is about 1 μm for fluorescence yield detection. Because of the high lateral resolution of the TEM, regions with different short-range order can be detected separately using EXELFS spectroscopy. However, a parallel EELS spectrometer is necessary for a quantitative data analysis.

Spektroskopische Methoden, die auf der elastischen Streuung von Photoelektronen basieren, die aus Festkörpern durch einen Anregungs-prozess erhalten werden können, erlauben eine elementspezifische Analyse der Materialien. Aus der numerischen Analyse von EXAFS und EXELFS Daten können Information über die Nahordnung oder über niedrig geordnete Bereiche gewonnen werden. Es werden vor allem Möglichkeiten und Probleme diskutiert, die bei der Strukturanalyse von Silizinmoxy-carbid-Matrices in Compositen, hergestellt durch Active Filler Controlled Pyrolysis (AFCOP), erwartet wurden. Die EXAFS Spektroskopie ergibt ein integrales Signal der Glasprobe, wobei die Informationstiefe für Fluoreszensdetektion ca. *1 μm beträgt. Aufgrund der hohen lateralen Auflösung des TEMs können mit Hilfe der EXELFS Spektroskopie Regionen mit unterschiedlichen Nahordnungen separat erfasst werden. Trotzdem ist ein paralleles EELS Spektrometer für eine quantitative Datenanalyse notwendig.*

Les méthodes spectroscopiques basées sur la dispersion élastique de photoélectrons, générés dans le solide par un procédé d'excitation, permettent l'analyse spécifique d'un élément du matériau. Des informations peuvent être obtenues quant à l'ordre à courte distance de régions désordonnées dans des composites céramiques, via l'analyse numérique des données EXAFS et EXELFS. En particulier, cet article traite des possibilités et problèmes que l'on peut attendre des analyses de structure de matrices silico-oxy-carbures dans des composites fabriqués par pyrolyse contrôlée d'une charge réactive. La spectroscopie EXAFS donne un signal intégral de l'échantillon vitreux, dont l'information correspond à une profondeur d'analyse d'environ 1 μm. Grâce à la haute résolution latérale du MET, des régions caractérisées par des ordres à courte distance différents peuvent être détectées séparément en utilisant la spectroscopie EXELFS. Cependant, un spectromètre EELS muni d'un détecteur à configuration parallèle est nécessaire pour une analyse quantitative des données.

1 Introduction

Strengthening of ceramic materials can be realized by various fabrication routes, e.g. conventional powder metallurgical technique, melt infiltration, chemical vapour infiltration, reaction-based processing or polymer pyrolysis. Relationships between technology, microstructure and macroscopic properties of ceramic composites are widely discussed in the literature, but the strength of these materials also depends on their atomic structure. Consequently, there exists a clear relevance for structure investigation methods that give information about the short-range order of ill-ordered regions in com-

Journal of the European Ceramic Society 0955-2219/92/$5.00 © 1992 Elsevier Science Publishers Ltd, England. Printed in Great Britain

posites, e.g. covalent-amorphous networks in advanced materials derived from silicon-containing pre-ceramic polymers.

Active Filler Controlled Pyrolysis (AFCOP) for fabrication of multiphase ceramic matrix composites is a new processing technique that consists of mixing appropriate active filler material with organometallic polymers and a subsequent pyrolysis.[1] In principle, the kinetics of the polymer pyrolysis and the formation of the microstructure can be controlled by kind, content and structure of the incorporated filler additive. Optimizing the filler systems, a shrinkage-controlled reaction pyrolysis seems to be possible.[2,3] At present, there is an important question for this new class of materials. How are the carbon atoms bound in the composite matrix after the pyrolysis and, consequently, is it justified to use the term 'oxycarbide glass'?

The discussion of effective investigation methods for the analysis of the atomic structure in ceramic composites prepared by the AFCOP technique can build on the knowledge about the structure analysis of Nicalon fibres. Nicalon fibres, fabricated by Nippon Carbon using the pyrolysis technique, consist predominantly of SiC, but their properties are influenced by additional phases. Up to now, it has not been completely understood how the oxygen atoms are built into the network and how the properties of the fibres are influenced. In addition to the conventional X-ray diffractional analysis, some structural investigation methods (e.g. XPS, IR, NMR, EXAFS) were used to obtain information about the bonding and the atomic short-range order, respectively.[4,5] The existence of a silicon oxycarbide phase is already known from the oxidation of SiC.[6] Recently, this phase was discussed for Nicalon fibres on the basis of XPS studies and a thermodynamical approach.[4]

The aim of this paper is to demonstrate the possibilities and limits of two structure characterization methods that are based upon the elastic scattering of photoelectrons and that are sensitive to the short-range order of polymer-derived oxycarbide glasses and glass ceramics: EXAFS spectroscopy (*E*xtended *X*-Ray *A*bsorption *F*ine *S*tructure) and EXELFS spectroscopy (*EX*tended *E*lectron Energy *L*oss *F*ine *S*tructure).

2 Relationship between Atomic Short-range Order and EXAFS/EXELFS

EXAFS and EXELFS stand for the extended fine structures in the X-ray absorption spectrum (XAS)

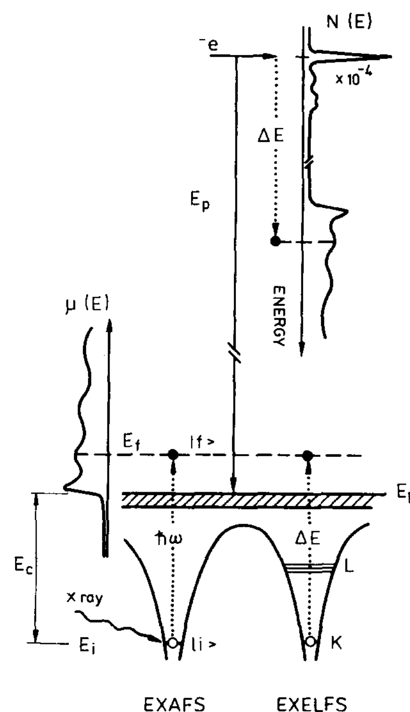

Fig. 1. Excitation of core electrons as well as schematic XAS and EELS spectra.

and in the electron energy loss spectrum (EELS) of a sample, i.e. the modulations within a region between about 30 eV and some hundred eV above the ionization energy of a core electron.[7,8]

The ionization of an atom, i.e. the excitation of a core electron at an energy level above the Fermi energy E_F, can result either from the absorption of an X-ray photon or from the energy loss of a primary electron. In both cases, ionization edges (absorption edges and loss edges, respectively) occur in the XAS and EELS spectra. The microscopical interpretation of the EXAFS and EXELFS modulations does not depend on the cause of the ionization (Fig. 1): an X-ray photon with the energy $\hbar\omega$ or a primary electron with the energy E_i knock out a core electron (binding energy E_c) that leaves the atom as a spherical wave (transition of an electron from initial state /i> of the energy E_i to a final state /f> of the energy E_f). The photoelectron wave outgoing from the ionized atom A is partially backscattered at the potentials of the neighbouring scattering atoms. The interference of outgoing and backscattered waves depend on the kinetic energy E_{kin} of the photoelectron and on the geometrical arrangement and the type of the scattering atoms. The modified final state /f⟩ of the electron results in a maximum (minimum) in the EXAFS and EXELFS region of the XAS and EELS spectra, respectively, in the case of positive (negative) interference (Fermi's Golden Rule).

The relationship between the structure parameters of the sample and the extended fine structure in a XAS or EELS spectrum can be defined analytically according to the model used. The total modulation $\chi_A(k)$ is a weighted sum of single oscillations, whereby the summation is performed over regions with different short-range order environments of the central atom and over the considered scattering atoms S. The weightings factors p_i/A are distribution coefficients of central atoms at sites with different short-range order environment i. In the case of composites, i denotes the different phases of the material.

Within the approximation of plane photoelectron waves and without consideration of multiple scattering effects, the EXAFS and EXELFS modulations above the K ionization edges (excitation of a 1s electron) are given as a function of the wave number k by

$$\chi_A(k) = \sum_{i,s(j)} p_{i/A} \cdot \chi^{s(j)}_{A/i} \quad (1)$$

$$\chi^{s(j)}_{A/i}(k) = -\frac{N^{s(j)}_{A/i}}{k \cdot (R^{s(j)}_{A/i})^2} \cdot |f^s(\pi, k)| \times \exp(2(\sigma^{s(j)}_{A/i})^2 k^2) \times \exp(-2R^{s(j)}_{A/i}/\lambda_e) \times \sin(2k \cdot R^{s(j)}_{A/i} + 2\delta_{p,A}(k) + \psi^s(\pi, k)) \quad (2)$$

$R^{s(j)}_{A/i}$ denotes the radius of the jth coordination shell at which are located $N^{s(j)}_{A/i}$ scattering atoms S (characterized by atomic number Z). $N^{s(j)}_{A/i}$ stands for the coordination number.

The experimental damping factors characterize thermal effects (Debye–Waller factor) and losses caused by inelastic scattering of photoelectrons. $(\sigma^{s(j)}_{A/i})^2$ stands for the average quadratic relative displacements of the atoms, λ_e for the average free path length of the photoelectrons. The quantum mechanical scattering process of the photoelectrons at the atomic potentials is described by central atom and backscattering phase $\delta_{p,A}(k)$ and $\psi^s(\pi, k)$ as well as by the backscattering amplitude $/f^s(\pi, k)/$. In the far-edge energy region, the wavenumber k of the photoelectron results from the dispersion relation of free electrons.

If spherical photoelectron waves are supposed and multiple scattering effects are considered, eqn (2) will become more complex.[9–15] In each case, this expression contains three material specific parameters for each coordination shell: N, R and σ^2.

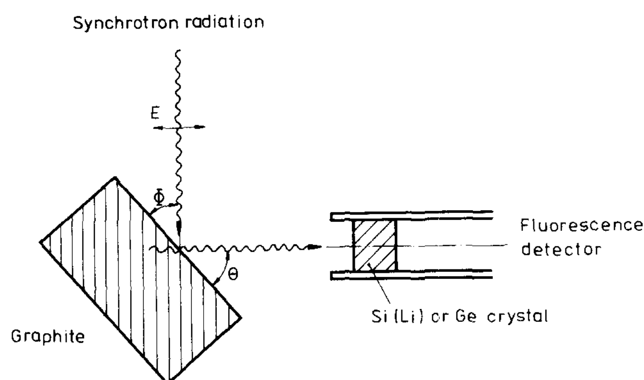

Fig. 2. The experimental setup showing schematically FY detection.

3 Experimental Details

3.1 Detection of fluorescence yield spectra

The most commonly used method of measuring the X-ray absorption spectra of concentrated samples has been the transmission method. However, in particular in the soft X-ray region it is difficult to prepare the suitable thin foils necessary for use with this technique. The fluorescence yield (FY) method of detecting EXAFS is an alternative possibility for obtaining bulk information of the sample. A typical experimental setup is shown schematically in Fig. 2.[16,17] The monochromatized synchrotron radiation hits the sample with an incidence angle Φ, the fluorescence photons are detected using a solid-state detector under an angle Θ.

The normalized FY spectrum of a graphite sample as a function of the energy of the incident photons is shown in Fig. 3 around the C K edge.[18] The experiment was performed at the storage ring BESSY using the plane grating grazing incidence monochromator HE-PGM-2. Typical beam conditions were 755 MeV electron energy and 150–450 mA ring current. The flux of monochromatized synchrotron radiation was monitored by a high-transmission gold grid. The detected photo current

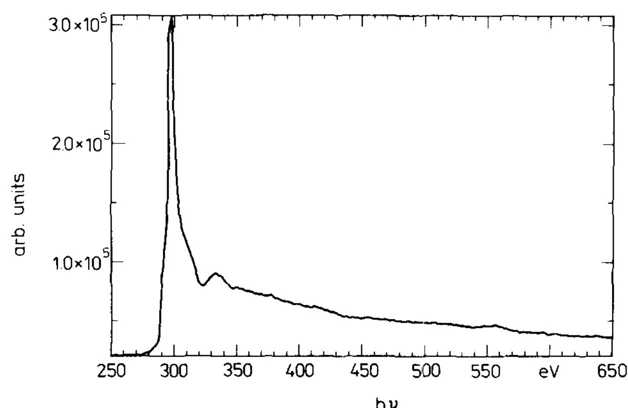

Fig. 3. Normalized FY spectrum of graphite ($T = 77$ K).

is proportional to the number of incident photons and, therefore, it could be used for normalization of the raw experimental data. The geometrical arrangement was chosen so that $\Phi = 85°$ and $\Theta = 5°$. The fluorescence photons were detected by a windowless Si(Li) detector.

In the case of a SiC_xO_y glass, an additional edge would occur at about 532 eV (O K edge). The energetic resolution of a solid-state detector allows the detection of only C K_α photons (277 eV). However, a breakdown of the C K_α FY occurs at the O K edge, whereby the intensity of the breakdown depends on the geometry factor $g = \sin\Phi/\sin\Theta$. The breakdown can be minimized for large Φ values (normal incidence of the primary radiation). For concentrated samples, however, the EXAFS amplitudes are incorrect as a result of the self-absorption effect. Consequently, errors occur in the extracted coordination numbers and Debye–Waller factors.[17,19,20]

Plane samples (about 1 cm^2) with a low roughness are necessary for FY measurements.

3.2 Detection of electron energy loss spectra

EELS spectroscopy, as a special branch of analytical transmission electron microscopy (ATEM), is favoured for components with low atomic number. In contrast to EXAFS spectroscopy, the element-specific information about the atomic short-range order can be gained with a high lateral resolution using the EXELFS spectroscopy. Object regions up to 10 nm can be resolved by optimizing the magnification and the spectrometer entrance aperture.

Commercially available analytical transmission electron microscopes (basic device) at which an EELS spectrometer is flanged can be used for EELS measurements.

A simplified scheme of a transmission electron microscope with a serial EELS spectrometer is shown in Fig. 4. The basic principle of an EELS detection system consists in a conversion of the energy distribution of the primary radiation modified in the sample in a three-dimensional intensity distribution. In the case of a serial spectrometer, the spectrum is electromagnetically scanned over an adjustable selector aperture and usually detected by a photomultiplier. In systems with parallel detection (PEELS), the spectrum is recorded simultaneously using position sensitive detectors (e.g. photodiode arrays, CCDs (charge coupled devices)).

From the theoretical point of view, EXELFS is exactly equal to EXAFS if multiple contributions can be suppressed experimentally.[21] For appli-

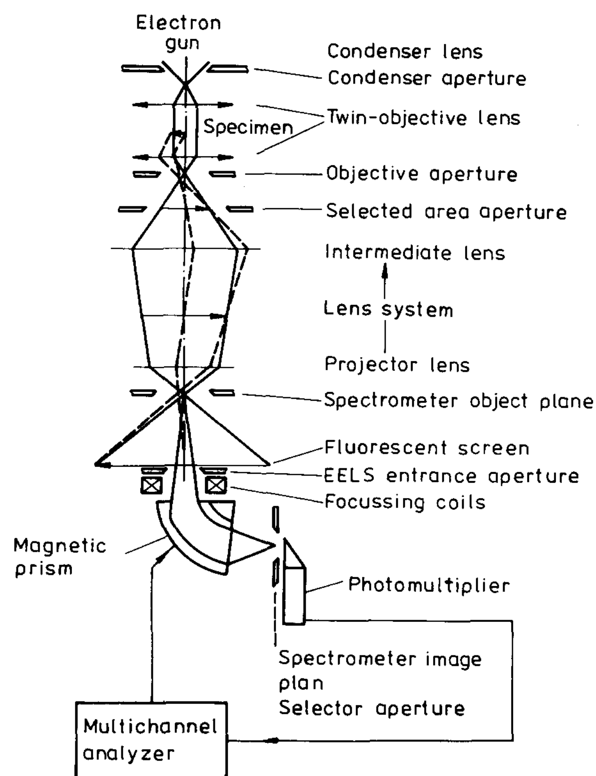

Fig. 4. The experimental setup showing schematically EELS detection.

cation of eqn (2) (dipole approximation) for the EXELFS analysis, a limitation of the convergence angle of the primary electrons (using the condenser aperture) and of the acceptance angle (using the objective aperture) with $\leqslant 10$ mrad is necessary.[22] Consequently, the intensity of the detector signal is limited. Using the microprobe mode, the resulting maximum values for both the condenser aperture and the objective aperture (for a focal length of the objective lens of 2·7 mm) are 50 μm.

An EELS spectrum of amorphous carbon that was recorded with the ATEM Philips CM-30 and a serial EELS spectrometer Gatan-607 at the Department of Material Science of the Mining Academy Freiberg is shown in Fig. 5.[23] The used object area was about 0·1 μm in diameter. A step width of 1 eV was used for recording the serial EELS spectrum. A measuring time of 40 ms per channel was chosen and 150 scans recorded, i.e. after accumulation, a total measuring time per channel of 6 s was obtained. The intensity above the C K edge amounted to about 10^4 counts and the energetic resolution was 2·5 eV.

A quantitative analysis of the EXELFS, however, requires at least 10^6 counts per energy channel, which would result in measuring times of several days in the case of a serial EELS spectrometer. That means that the demand of good statistics of the spectra in reasonable measuring times can be

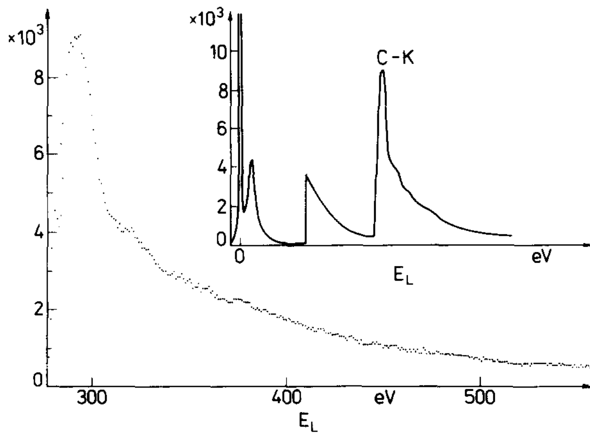

Fig. 5. EELS spectrum of amorphous carbon.

fulfilled only insufficiently. Commercial spectrometers that use parallel detection with a position sensitive detector meet this demand much better.[24-26]

Assuming identical conditions for recording, a comparable quality of the EXELFS spectra demands a measuring time and an electron dose which are 10^2 to 10^3 times higher for serial detection than in the case of parallel detection. In comparison with serially detected spectra, the statistical inaccuracy can be improved by a factor of $n^{1/2}$ (n = number of channels) in the spectra that are recorded using the parallel detection.[27] This means that radiation damage which can occur after long ray-treatment—not only in polymers but also in inorganic materials—is also reduced using simultaneous recording.

To avoid plural losses of the primary electrons in the sample, samples with a very low thickness are necessary for the EELS spectroscopy. In addition, the ionization edges are convoluted with the plasmon losses (energy region 0–50 eV), and, consequently, the average free path length λ_{pl} between two plasmon excitations are a measure for the maximum sample thickness. Typical sample thicknesses should amount to some 10 nm. However, samples with a 10 times larger sample thickness can be used if a deconvolution of the spectra is performed.[8,28]

A combined mechanical preparation by cutting and grinding as well as a subsequent ion milling could be favoured for the sample preparation of the relatively brittle glass matrices for EELS studies.

A sample prepared by the AFCOP technique (initial polymer: commercial polymethylphenylsiloxane, pyrolysis at 1400°C/4 h) was cut mechanically. Subsequently, small plates with a maximum area of 1 mm² were ground manually to a thickness of about 100 μm and stuck to a copper blend. Then the sample was thinned on both sides in a Gatan Duomill 600 using Ar gas. The chosen accelerative voltage was 6 kV, the angle of incidence was between 10° and 25°. EELS spectra of this AFCOP sample and, for comparison, of crystalline SiC, are shown in Fig. 6. Already for intensities of $\leqslant 10^4$ counts, significant differences can be noticed above the C K edge.

4 Data Analysis

The first step of the data analysis includes the extraction of the $\chi_{A,\mathrm{exp}}(k)$ data from the experimental primary data. In the case of FY spectra, it means

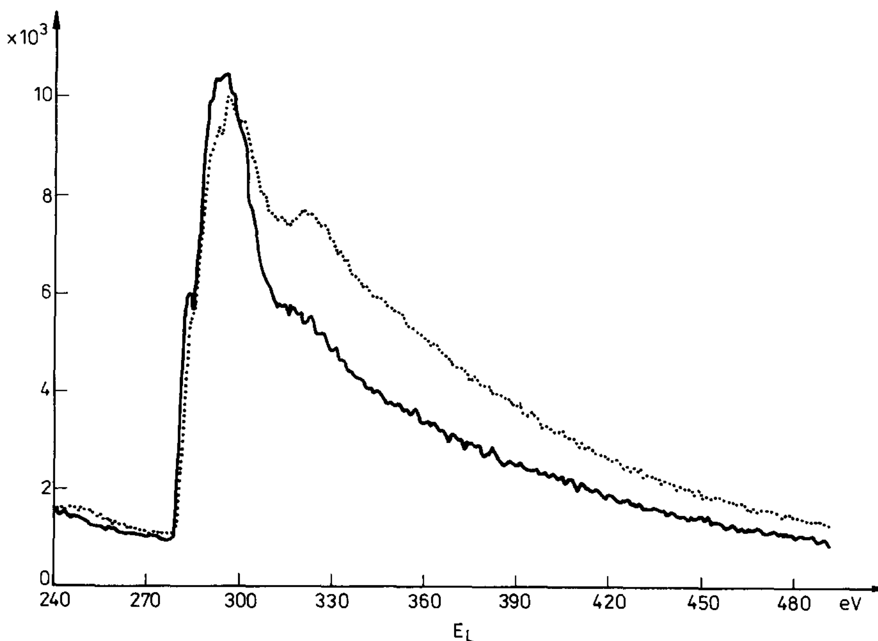

Fig. 6. EELS spectrum of a glass prepared by the AFCOP technique (——) and, for comparison, of SiC (······).

normalization, fixing the energy zero, transformation of the E scale into the k scale and separation of the monotonous background. In the case of EELS spectra, the normalization is not necessary, but, in general, a deconvolution of the spectra has to be done. The second step of the data analysis is based upon the extracted $\chi_{A,\exp}(k)$ data and is—on condition that the dipole approximation can be used—independent of the type of excitation and detection.

Because the $\chi_A(k)$ modulation represents a superposition of periodical oscillations, it is useful to carry out a Fourier expansion of the fine structure. This Fourier transformation (partial radial atomic distribution function, PRDF) gives qualitative information about the atomic short-range order in the environment of the ionized atom. However, the position and height of the peaks are influenced by the quantum mechanical scattering quantities.

For a quantitative data analysis, it is favourable to perform it either with the 'experimental' fine structure or with the interesting contribution of the PRDF after an inverse Fourier transform in the k space. The free parameters in the model function (EXAFS formula) are determined by the use of a special least-squares algorithm in such a way that the fit to the 'experimental' data is as good as possible. For each coordination shell, at least three parameters of the model have to be considered: the coordination number N, the radius of the coordination shell R and the mean square relative displacement of emitting and scattering atoms σ^2. To this an energy shift parameter E_0 has to be added which considers the difference between the energy zero extracted from the experimental X-ray absorption spectrum (first inflection point) and the muffin-tin zero of the core electron.

Often, however, the model contains too many free parameters compared with the restricted number of uncorrelated details in the experimental spectrum. Then, the problem is mathematically ill-conditioned and it is not possible to obtain a unique solution of the minimizing procedure.[29] A reduction of the effective number of free parameters is possible by the use of the Bayesian strategy in such a way that several experimental signals and as much pre-information as possible are combined in the same loss function. In contrast to other regularization mechanisms used, e.g. the Tikhonov regularization,[30] the weighting factors of the Bayesian strategy are based on physical reasons. These factors are reciprocal experimental errors for the experimental data and reciprocal confidence intervals for the considered constraints.[31,32] The original version of the Bayesian method was improved in such a way that implicit linear constraints between the parameters can be considered.[33,34] In particular, 'couplings' between p_i, N, R and σ^2 were used.

For a microphase decomposition in metallic glasses it has been shown that the Bayesian strategy can be applied to the EXAFS analysis of multiphase systems.[35–37] In particular, $p_{i/A}$ parameters were determined. The phase fractions p_i could be obtained using the following relations:

$$\sum_i p_{i/X} = 1 \tag{3}$$

$$\sum_X p_{i/X} * p_X = p_i \tag{4}$$

$$X = \{A, B, \ldots\}$$

p_X and p_i denote the atomic concentration of the component X (e.g. A) in the composite material and the fraction of the phase i, respectively.

On the other hand, EXELFS spectra of the individual phases i of the composite material can be detected with the high lateral resolution of the ATEM. Thus, all central atoms that contribute to such an EXELFS spectrum have the same short-range order environment and, consequently, the summation in eqn (1) has to be performed only for the considered coordination shells j. The opportunity of a structural characterization separately for different phases is one significant advantage of EXELFS spectroscopy in contrast to EXAFS spectroscopy which gives only integral information.

For the EXAFS and EXELFS analysis, another problem has to be considered. Undisturbed energy regions of some hundred electron volts above the ionization edge are necessary for an analysis of the extended fine structure. This demand is fulfilled for X-ray absorption spectra above the K ionization edges of heavy elements, because the energy difference between the K edges of $3d$ transition-metal elements are juxtaposed in the periodic table by amounts of at least 500 eV. However, the distances between the K edges of light elements with consecutive atomic number is significantly lower (e.g. only 118 eV between C K and N K edges). In addition, it has to be checked if the energies of L and M edges of heavy elements are within the EXAFS or EXELFS region above the K edges of light elements (Fig. 7). Such edges can make an analysis extremely difficult or impossible.

The suppression of FY contributions that are separated by more than 120–150 eV is possible in principle with efficient Si(Li) and Ge solid-state

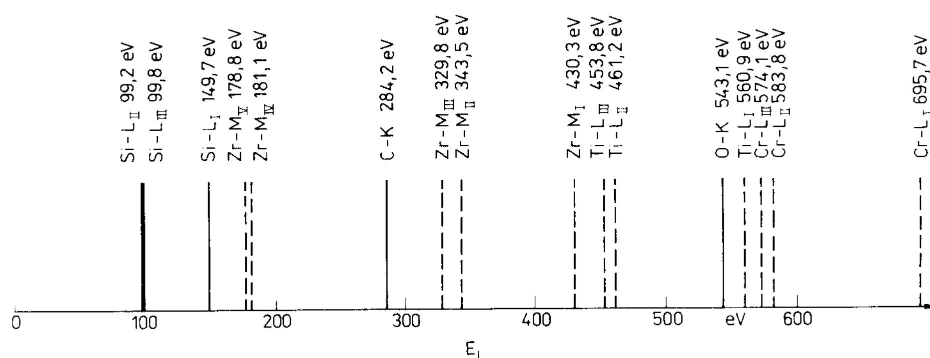

Fig. 7. Energies of ionization edges of silicon oxycarbide glasses and of typical filler components (- - -).

detectors. However, drops of the FY signal occur at the 'suppressed' contributions. The intensity of these drops can be minimized by choosing a favourable detection geometry; however, the amplitudes of the EXAFS wiggles are reduced too.[17]

5 Conclusions

In principle, both EXAFS and EXELFS spectroscopy are suitable methods for short-range order characterization of glass matrices derived from polymers if a FY detector and a parallel EELS spectrometer are used. On condition that 'undisturbed' energy regions of some hundred electron volts above the ionization edge can be analysed, the accuracy of the determined interatomic distances (nearest neighbours) amounts to about 0·02 Å, whereas the relative error for the coordination numbers and Debye–Waller factors amounts to about 20%. For both methods, disturbing ionization edges can occur within the relevant energy range. They can be suppressed to some extent in FY measurements by choosing a proper geometry of the experiment.

Using an ATEM, EELS spectra can be detected with a high lateral resolution, and an additional characterization of the sample region is possible by a microscopic picture. The problems of EXELFS spectroscopy are above all the existence of multipole transitions and, consequently, an angle-dependent fine structure as well as possible plural losses.

Finally it should be mentioned that the shape of the ionization edges and their shift (chemical shift) also give information about the bonding. So, the formation of energy gaps as a consequence of the metal–oxide transition (e.g. $Al \rightarrow Al_2O_3$, $Si \rightarrow SiO_2$) result in a shift of the ionization edge of the metallic component to higher energies (some eV).

Summing up, it can be said that EXAFS and EXELFS spectroscopy are powerful methods for the structure analysis of glasses, but complete structure models can be obtained only if these techniques are used in combination with other investigation methods (e.g. IR, Raman, NMR or Mößbauer spectroscopy).

Acknowledgement

The authors wish to thank Prof. Dr P. Greil and Dipl.-Ing. M. Seibold (TU Hamburg–Harburg) for making available the samples prepared by the AFCOP technique as well as for valuable discussions.

References

1. Seibold, M. & Greil, P., Composite ceramics from polymer–metal mixtures. In *1st European Conference on Advanced Materials and Processes*, Aachen, 1989.
2. Greil, P. & Seibold, M., Active filler controlled pyrolysis (AFCOP)—a novel processing route to ceramic matrix composites. In *2nd Int. Ceram. Sci. and Technol. Congr.*, Orlando, 1990.
3. Erny, T., Seibold, M., Jarchow, O. & Greil, P., Microstructure of polymer derived oxycarbide composites, *J. Am. Cer. Soc.*, submitted.
4. Porte, L. & Sartre, A., *J. Mater. Sci.*, **24** (1989) 271.
5. Laffon, C., Flank, A. M., Lagarde, P., Laridjani, M., Hagege, R., Olry, P., Cotteret, J., Dixmier, J., Miquel, J. L., Hommel, H. & Legrand, A. P., *J. Mater. Sci.*, **24** (1989) 1503.
6. Pampuch, R., Ptak, W., Jonas, S. & Stoch, J., *Mater. Sci. Monographs*, **6** (1980) 435.
7. Teo, B. K., *EXAFS—Basic Principles and Data Analysis*. Springer-Verlag, Berlin, 1986.
8. Egerton, R. F., *Electron Energy Loss Spectroscopy in the Electron Microscope*. Plenum Press, New York, 1986.
9. Sayers, D. E., Stern, E. A. & Lytle, F. W., *Phys. Rev. Lett.*, **27** (1971) 1204.
10. Schaich, W. L., *Phys. Rev. B*, **27** (1983) 6489; *Phys. Rev. B*, **29** (1984) 6513.
11. Gurman, S. J., Binsted, N. & Ross, I., *J. Phys. C*, **17** (1984) 143; *J. Phys. C*, **19** (1986) 1845.
12. Barton, J. J. & Shirley D. A., *Phys. Rev. B*, **32** (1985) 1019; *Phys. Rev. B*, **32** (1985) 1892; *Phys. Rev. B*, **32** (1985) 1906.
13. Rehr, J. J., Albers, R. C., Natoli, C. R. & Stern, E. A., *J. Phys.*, **47** (1986) 1845.
14. Fritzsche, V. & Rennert, P., *Phys. Stat. Sol. (b)*, **135** (1986) 49; *Phys. Stat. Sol. (b)*, **142** (1987) 15.
15. Rennert, P. & Hung, N. V., *Phys. Stat. Sol. (b)*, **148** (1988) 49.
16. Arvanitis, D., Döbler, U., Wenzel, L., Baberschke, K. & Stöhr, J., *J. Phys.*, **47** (1986) C8–173.

17. Zschech, E., Tröger, L., Arvanitis, D., Michaelis, H., Grimm, U. & Baberschke, K., *Solid State Commun.*, **82** (1992) 1.
18. Zschech, E., Michaelis, H., Grimm, U. & Tröger, L., unpublished.
19. Tröger, L., Arvanitis, D., Rabus, H., Wenzel, L. & Baberschke, K., *Phys. Rev. B*, **41** (1990) 7297.
20. Tröger, L., Arvanitis, D., Röhler, J., Schliepe, B. & Baberschke, K., *Solid State Commun.*, **79** (1991) 479.
21. Stern, E. A., *J. Phys.*, **47** (1986) C8-3.
22. Fink, J., Recent developments in energy loss spectroscopy. *Adv. Electronics Electron Physics*, **75** (1989) 121.
23. Klemm, V. & Zschech, E., unpublished.
24. Disko, M. M. & Shuman, H., *Ultramicroscopy*, **20** (1986) 43.
25. Johnson, D. E. & Connick, M., *Rev. Sci. Instr.*, **58** (1987) 1822.
26. Krivanek, O. L., Ahn, C. C. & Keeney, R. B., *Ultramicroscopy*, **21** (1987) 87.
27. Reimer, L., *Energieverlustspektroskopie und Energiefilterung in der TEM*. Münster, 1987.
28. Leapman, R. D. & Swyt, C. R., In *Analytical Electron Microscopy—1981*, ed. R. H. Geiss. San Francisco Press, San Francisco, 1981, p. 164.
29. Hofmann, B., *Regularization for Applied Inverse and Ill-Posed Problems*. B. G. Teubner, Leipzig, 1986.
30. Tikhonov, A. N. & Arsenin, V. Ya. In *Solution of Ill-Posed Problems, Scripta Series in Mathematics*. John Wiley and Sons, New York, 1977,
31. Bandemer, H., *Theorie und Anwendung der optimalen Versuchsplanung*, Vol. 1, Akademie-Verlag, Berlin, 1977.
32. Pilz, J., *Bayesian Estimation and Experimental Design in Linear Regression Models*. B. G. Teubner, Leipzig, 1983.
33. Blau, W., Zschech, E. & Bergmann, J., *Nucl. Instr. Meth. A*, **261** (1987) 166.
34. Blau, W. & Zschech, E., *Phys. Stat. Sol.*, **129** (1992) 69.
35. Zschech, E., Blau, W., Kleinstück, K., Hermann, H., Mattern, N., Kozlov, M. A. & Sheromov, M. A., *J. Non-Cryst. Solids*, **86** (1986) 336.
36. Zschech, E., Blau, W., Fjodorov, V. K. & Sheromov, M. A., *Nucl. Instr. Meth. A*, **282** (1989) 586.
37. Zschech, E. & Blau, W., EXAFS investigation of microphase decomposition in metal–metalloid glasses. In *Amorphous Structures—Methods and Results*, ed. D. Schulze. Akademie-Verlag, Berlin, 1990, p. 179.